Preprints of the 21st IFAC World Congress (Virtual)
Berlin, Germany, July 12-17, 2020

Co-design of a Continuously Variable Transmission using Sequential Quadratic Programming-based Control Optimization

C.A. Fahdzyana M.C.F. Donkers T. Hofman

Eindhoven University of Technology, Netherlands
(e-mail: c.a.fahdzyana@tue.nl,m.c.f.donkers@tue.nl).

Abstract: For systems with nonlinear dynamics, Dynamic Programming for control is commonly considered in the framework of integrated plant and control system design. Despite its popularity, this control strategy can run into some computational issues as the performance is dependent on the state and input discretization. In this paper, we propose a Sequential Quadratic Programming-based control optimization strategy for integrated system design, where both the plant and control are optimized for the case study of a continuously variable transmission. The proposed plant and control design problem will be solved using a nested strategy.

Keywords: Multi-objective optimization, optimization, optimal control, co-design, sequential quadratic programming

1. INTRODUCTION

In the current time, vehicles with high energy efficiency as well as low cost of ownership are desired. One way to improve vehicle driveline efficiency is by utilizing a continuously variable transmission (CVT). Unlike other types of transmissions, a CVT has continuous speed ratio values, which allow the engine or electric machine to be operated close to, if not at, the most optimal operating points. Compared to other types of vehicle transmissions, CVTs have the potential to improve the overall vehicle powertrain efficiency as well as the driving comfort.

For most automotive applications, CVTs with higher power capacity, reduced mass and size are needed to compete with other types of transmissions (Brandsma, 1999). This gives the motivation to redesign the existing CVT design which can be approached using integrated plant and control design (co-design).

Generally, co-design methods can be classified into several strategies, namely sequential, iterative, nested/bi-level, and simultaneous (Fathy, 2003). Traditionally, system design is done in sequential or iterative manner due to their ease of practical implementations. Nevertheless, these methods can not guarantee optimality in the obtained design (Fathy, 2001; Peters, 2009). Because of this, nested and simultaneous methods are preferred for integrated plant and control design.

The nested approach is proposed as an alternative to the simultaneous design optimization method. This strategy consists of an outer loop which optimizes for the plant design parameters, while the inner loop seeks for the optimal control solution given the plant design parameters passed by the outer loop. A special case of nested co-design is when the control problem can be formulated as a linear-quadratic regulator or linear-quadratic dynamic optimization, which yields an efficient solution to the control (inner) loop (Herber, 2018).

For systems with nonlinear dynamics, open-loop control strategies are commonly considered in the framework of co-design. Among the control strategies, the use of Dynamic Programming (DP) to solve nonlinear control problems in the field of co-design has been widely implemented, such as (Perez, 2006; Sundstrom, 2008; Silvas, 2014). This is due to the ability of DP to provide the optimal control input trajectory for systems with nonlinear dynamics. However, DP's performance depends on not only the length of the optimization horizon, but also on the state and input discretization, which may result in a much higher computational time for multiple input and state variables (Bellman, 1957). As the computational cost of nested co-design depends on the computation time needed to solve the control optimization, effective formulation of the control design problem can significantly benefit the computational cost of integrated system design using nested approach.

In this paper, an integrated plant and control system design for a CVT system is performed. The goal is to achieve a new CVT design with lower variator mass without compromising the required performance for driving. In this case, the design problem is nonlinear due to the objective function as well as the system dynamics. The control optimization problem will be solved by a Sequential Quadratic Programming (SQP) based algorithm. Here, we select a control input such that the SQP-based algorithm can be applied for the system. The combined plant and control design optimization will be solved using a nested approach.

This paper is organized as follows. In Section 2, the necessary mathematical models for the problem of integrated plant and control system design of a CVT are presented. Following that, the design problem for CVT is formulated

in Section 3. The results and discussions of the proposed design strategy are elaborated in Section 4. Lastly, the conclusions and future extensions of this study are presented in Section 5.

2. SYSTEM MODELING

In this section, we will present the modeling of relevant components and subsystems for the integrated system design of a Continuous Variable Transmission (CVT).

2.1 CVT variator model

A typical CVT variator consists of two pulley sheaves on the primary side (connected to the engine or EM) and the one on secondary side (connected to the wheels). The CVT geometric ratio is given by:

$$r_{\mathrm{g}} = \frac{R_{\mathrm{p}}}{R_{\mathrm{s}}} = \frac{\omega_s}{\omega_{\mathrm{p}}}\,, \tag{1}$$

where ω_{p} and ω_s are the primary and secondary rotational speed, R_{p} and R_{s} are the primary and secondary running radius, which is the distance of the belt contact point from the corresponding pulley center points, as shown in Fig. 1.

Here, the ratio dynamics of the CVT is described by the Carbone-Mangialardi-Mantriota (CMM) shifting dynamics model, which is given by Carbone (2005):

$$\dot{r}_{\mathrm{g}} = 2\omega_{\mathrm{p}}\Delta\frac{1+\cos^2(\beta)}{\sin(2\beta)}c(r_{\mathrm{g}})\left[\ln\frac{F_{\mathrm{p}}}{F_{\mathrm{s}}} - \ln\frac{F_{\mathrm{p}}}{F_{\mathrm{s}}}\Big|_{ss}\right] \tag{2}$$

where ω_{p} is the primary rotational speed, Δ is pulley deformation, $\frac{F_{\mathrm{p}}}{F_{\mathrm{s}}}$ is the clamping force ratio, and $\frac{F_{\mathrm{p}}}{F_{\mathrm{s}}}\big|_{ss}$ is the steady-state clamping force ratio, which is the value needed to sustain a certain ratio value. Usually, the primary clamping force is controlled to provide the desired ratio tracking performance, while the secondary clamping force is controlled to ensure safe operation of the transmission. The secondary clamping force to provide a safe torque transfer is adopted from (Vroemen, 2001):

$$F_{\mathrm{s}} = \frac{\cos(\beta)\cdot(|T_{\mathrm{p}}| + S_f\cdot T_{\mathrm{p,max}})}{2\mu_{\mathrm{cvt}}R_{\mathrm{p}}}\,. \tag{3}$$

where T_{p} denotes the primary torque, $T_{\mathrm{p,max}}$ is the maximum engine torque, μ_{cvt} is the traction coefficient, and S_f is the safety factor, which is typically selected to be 30%. The shifting dynamics term $c(r_{\mathrm{g}})$ is expressed as a quadratic function of r_{g} (Fahdzyana, 2020),

$$c(r_{\mathrm{g}}) = c_1 r_{\mathrm{g}}^2 + c_2 r_{\mathrm{g}} + c_3\,, \tag{4}$$

where the coefficients are given in Table 1. The steady state clamping force ratio depends on the pulley wedge angle as well as the transmission load torque. Here, the steady-state clamping force ratio is approximated as a function of ratio r_{g}, wedge angle β, and torque ratio Υ,

$$\frac{F_{\mathrm{p}}}{F_{\mathrm{s}}}\Big|_{ss} = a_1(\beta)r_{\mathrm{g}}^2 + a_2(\beta)r_{\mathrm{g}} + a_3(\beta) + b_1\Upsilon^2 + b_2\Upsilon\,. \tag{5}$$

where $b_1 = 1.4741$, $b_2 = 0.4088$. The coefficients a_i of the model in (7) depend on the wedge angle β as follows

$$a_i(\beta) = a_{i1}\beta^2 + a_{i2}\beta + a_{i3}\,, \tag{6}$$

where $i \in \{1,2,3\}$. The fitted parameters are summarized in Table 1.

The torque ratio Υ denotes the torque ratio, given by (Meulen, 2010)

$$\Upsilon = \frac{T_{\mathrm{p}}}{|T_{\mathrm{p}}| + S_{\mathrm{f}}\cdot T_{\mathrm{p,max}}}\,, \tag{7}$$

which describes the ratio between the actually transmitted divided by the torque that is maximally transmitted (without large slip values at the variator).

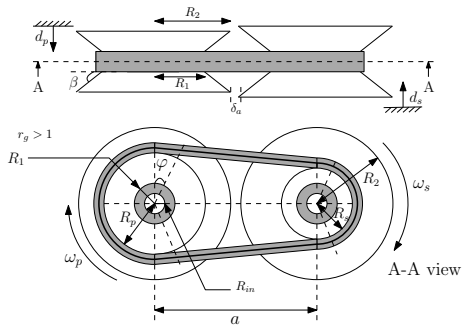

Fig. 1. CVT variator diagram

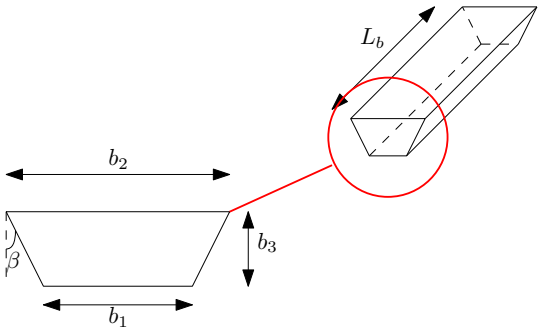

Fig. 2. V-belt parameters

2.2 Variator Mass Model

One of the objectives in the plant and controller co-design problem is to minimize the CVT variator mass. This mass can be formulated as a function of the pulley sheaves and transmission belt dimensions and is given by

$$M_{\mathrm{v}} = \rho_{\mathrm{pu}}V_{\mathrm{pu}} + \rho_{\mathrm{b}}V_{\mathrm{be}}\,, \tag{8}$$

where we have,

$$\begin{aligned} V_{\mathrm{pu}} = {} & \tfrac{2\pi}{3}(R_{2,\mathrm{p}} - R_{1,\mathrm{p}})\tan(\beta)(R_{2,\mathrm{p}}^2 + R_{1,\mathrm{p}}^2 + R_{1,\mathrm{p}}R_{2,\mathrm{p}}) \\ & + \tfrac{2\pi}{3}(R_{2,\mathrm{s}} - R_{1,\mathrm{s}})\tan(\beta)(R_{2,\mathrm{s}}^2 + R_{1,\mathrm{s}}^2 + R_{1,\mathrm{s}}R_{2,\mathrm{s}}) \end{aligned} \tag{9}$$

$$V_{\mathrm{be}} = \frac{b_1 + b_2}{2}\cdot b_3 \cdot L_{\mathrm{b}}\,, \tag{10}$$

with R_1 and R_2 are the pulley top and bottom radii, L_{b} is the belt length, b_1, b_2, and b_3 are the belt parameters, shown in Fig. 2.

3. PROBLEM FORMULATION

In this section, we formulate the (nonlinear) optimization problem for the integrated plant and control design

Table 1. Parameters

par.	value	par.	value	par.	value
a_{11}	11.9274	a_{12}	-5.6474	a_{13}	0.5647
a_{21}	-71.9417	a_{22}	31.3774	a_{23}	-2.9309
a_{31}	57.2683	a_{32}	-24.5247	a_{33}	3.2337
c_1	5.8553	c_2	2.8134	c_3	0.3832

problem of the CVT. The system design objective is to minimize the transmission variator mass, while simultaneously minimizing the clamping force and the error for ratio trajectory tracking. This is because the CVT energy consumption depends on the applied clamping forces. Furthermore, the maximum and minimum reachable transmission ratio $\overline{r_{\mathrm{g}}}$ and $\underline{r_{\mathrm{g}}}$ are defined by pulley parameters R_1 and R_2. To be more precise, the minimum and maximum reachable transmission ratio is given by,

$$\underline{r_{\mathrm{g}}} = \frac{R_{1,\mathrm{p}} + \delta_{\mathrm{in}}}{R_{2,\mathrm{s}} - \delta_{\mathrm{ou}}}\,,\ \overline{r_{\mathrm{g}}} = \frac{R_{2,\mathrm{p}} - \delta_{\mathrm{ou}}}{R_{1,\mathrm{s}} + \delta_{\mathrm{in}}}\,, \tag{11}$$

where δ_{ou} and δ_{in} is the maximum distance of the belt from the pulley edges. As the variator size is to be reduced, the maximum transmission ratio $\overline{r_{\mathrm{g}}}$ required for sufficient driving performance must therefore be realized by the new CVT design.

The combined optimization problem can be formulated as a minimization problem of a weighted sum of the corresponding plant and control design objectives J_{p} and J_{c}, i.e.,

$$\min w_{\mathrm{p}} \underbrace{M_v}_{J_{\mathrm{p}}} + w_c \underbrace{\int_{t_o}^{t_f} q\,(r_{g,r}(t) - r_{\mathrm{g}}(t))^2 + r\,u(F_{\mathrm{p}})^2\,\mathrm{d}t}_{J_{\mathrm{c}}}\,, \tag{12a}$$

in which w_{p} and w_c are positive weights that weigh the plant and control objective functions, $r_{g,r}$ and r_{g} are the desired and CVT ratio trajectory, respectively, and u is the control effort that is a function of the primary clamping force F_{p}, which will be explained in this section. Furthermore, q and r are the control weights that lead to a trade-off between accurate tracking error and control effort.

The minimization problem (12a) is solved subject to a set of plant design constraints, given by,

$$g_{p1,2} : \underline{\beta} \le \beta \le \overline{\beta}\,, \tag{12b}$$
$$g_{p3,4} : \underline{R_{1,\mathrm{p}}} \le R_{1,\mathrm{p}} \le \overline{R_{1,\mathrm{p}}}\,, \tag{12c}$$
$$g_{p5,6} : \underline{R_{2,\mathrm{p}}} \le R_{2,\mathrm{p}} \le \overline{R_{2,\mathrm{p}}}\,, \tag{12d}$$
$$g_{p7,8} : \underline{R_{1,\mathrm{s}}} \le R_{1,\mathrm{s}} \le \overline{R_{1,\mathrm{s}}}\,, \tag{12e}$$
$$g_{p9,10} : \underline{R_{2,\mathrm{s}}} \le R_{2,\mathrm{s}} \le \overline{R_{2,\mathrm{s}}}\,, \tag{12f}$$
$$h_{p1} : R_{2,\mathrm{p}} - \overline{r_{\mathrm{g}}}\,R_{1,\mathrm{s}} = \overline{r_{\mathrm{g}}}\,\delta_{in} + \delta_{ou}\,, \tag{12g}$$
$$h_{p2} : R_{2,\mathrm{s}}\underline{r_{\mathrm{g}}} - R_{1,\mathrm{p}} = \underline{r_{\mathrm{g}}}\,\delta_{ou} + \delta_{in}\,, \tag{12h}$$

and control design constraints,

$$h_{c1} : \dot{r}_{\mathrm{g}} = 2\omega_{\mathrm{p}}\Delta\frac{1+\cos^2(\beta)}{\sin(2\beta)}c(r_{\mathrm{g}})\left[\ln\frac{F_{\mathrm{p}}}{F_{\mathrm{s}}} - \ln\frac{F_{\mathrm{p}}}{F_{\mathrm{s}}}\Big|_{ss}\right] \tag{12i}$$

$$g_{c1,2} : \underline{F_{\mathrm{p}}} \le F_{\mathrm{p}}(t) \le \overline{F_{\mathrm{p}}}\,. \tag{12j}$$

As the CVT losses depend on the clamping forces, it is desired to minimize the clamping force F_{p} that is required to perform ratio shifting. Consider the nonlinear dynamics in (12i), we select the state variable x as r_{g}, and the system control input u to be $\ln\frac{F_{\mathrm{p}}}{F_{\mathrm{s}}} - \ln\frac{F_{\mathrm{p}}}{F_{\mathrm{s}}}\big|_{ss}$. The reasoning behind it is because F_{s} and $\frac{F_{\mathrm{p}}}{F_{\mathrm{s}}}\big|_{ss}$ are given over time; thus, minimizing the term $\ln\frac{F_{\mathrm{p}}}{F_{\mathrm{s}}} - \ln\frac{F_{\mathrm{p}}}{F_{\mathrm{s}}}\big|_{ss}$ implies the minimization of F_{p}. We then have:

$$\dot{x} = 2\,\omega_{\mathrm{p}}\,\Delta\,\frac{1+\cos^2(\beta)}{\sin(2\beta)}c(x)u\,. \tag{13}$$

The actual primary clamping force F_{p} is then given by:

$$F_{\mathrm{p}} = \exp\left\{u + \ln\left(\frac{F_{\mathrm{p}}}{F_{\mathrm{s}}}\Big|_{ss}\right)\right\}\cdot F_{\mathrm{s}} \tag{14}$$

To solve the co-design optimization problem (12), we will propose a nested approach, which consists of an inner and outer loop. In the inner loop of the optimization problem, the (nonlinear) optimal control problem is solved for a given set of plant parameters, while at the outer loop, the plant parameters are optimized for the given controller. Since the inner loop involves solving a constrained nonlinear optimal control problem, an efficient approach will be presented below, which is based on sequential quadratic programming (SQP).

3.1 Co-design with SQP-based Control Optimization

The optimal control problem, i.e., optimization problem (12) in which β, $R_{1,\mathrm{p,s}}$ and $R_{2,p,s}$ are fixed, is nonlinear due to the nonlinear dynamics (2) and constrained due to limitations of the clamping force. In this paper, we propose to solve this nonlinear optimal control problem by reformulating it as a static optimization problem that is solved using sequential quadratic programming (SQP). In SQP, a nonlinear optimization problem is solved by recursively solving linear constrained quadratic programming problem by approximating the objective function with a quadratic formulation (Nocedal, 2006). The general formulation of the SQP algorithm is given by:

$$[x_{\mathrm{k}}^{i+1}, u_{\mathrm{k}}^{i+1}] = \underset{x_{\mathrm{k}},u_{\mathrm{k}}}{\operatorname{argmin}} \sum_{k=0}^{N-1} \frac{1}{2}\begin{bmatrix} x_{\mathrm{k}} - x_{\mathrm{k}}^i \\ u_{\mathrm{k}} - u_{\mathrm{k}}^i \end{bmatrix}^\top H_k \begin{bmatrix} x_{\mathrm{k}} - x_{\mathrm{k}}^i \\ u_{\mathrm{k}} - u_{\mathrm{k}}^i \end{bmatrix} + F_k^\top \begin{bmatrix} x_{\mathrm{k}} \\ u_{\mathrm{k}} \end{bmatrix}, \tag{15}$$

subject to linearized state dynamics,

$$x_{k+1} = f(x_{\mathrm{k}}^i, u_{\mathrm{k}}^i) + \nabla f(x_{\mathrm{k}}^i, u_{\mathrm{k}}^i)\begin{bmatrix} x_{\mathrm{k}} - x_{\mathrm{k}}^i \\ u_{\mathrm{k}} - u_{\mathrm{k}}^i, \end{bmatrix} \tag{16a}$$

as well as the linear state x and input u constraints,

$$\underline{x}_k \le x_{\mathrm{k}} \le \overline{x}_k \tag{16b}$$
$$\underline{u}_k \le u_{\mathrm{k}} \le \overline{u}_k \tag{16c}$$

where i is the optimization iteration $i \in \mathbb{R}$, k denotes the discretized timesteps for all $k \in \{0, 1, \ldots, N-1\}$, N is the length of optimization $N = \frac{t_f - t_o}{\Delta t}$, and Δt is the discrete time interval. Additionally, H_k is a positive semidefinite Hessian matrix, F_k is the matrix of the gradient, and $f(x, u)$ is the nonlinear plant dynamics. The termination criterion is selected for when the change of the cost function at the current and previous iteration is less than or equal to a certain tolerance, given by,

$$|J^{i+1} - J^i| \le \epsilon_{tol}\,. \tag{17}$$

Hence, the control objective in (12a) can be written as a quadratic objective formulation,

$$\underset{\mathbf{x},\mathbf{u}}{\operatorname{argmin}} \frac{1}{2}\begin{bmatrix}\mathbf{x}\\ \mathbf{u}\end{bmatrix}^\top \begin{bmatrix}\mathbf{Q} & \\ & \mathbf{R}\end{bmatrix}\begin{bmatrix}\mathbf{x}\\ \mathbf{u}\end{bmatrix} + \mathbf{F}^\top \begin{bmatrix}\mathbf{x}\\ \mathbf{u}\end{bmatrix} \tag{18}$$

where $\mathbf{x}$ and $\mathbf{u}$ are vectors of the discretized state and input variables, $\mathbf{x} = [x_0, x_2, ..., x_N]^\top$, $\mathbf{u} = [u_0, u_2, ..., u_{N-1}]^\top$, $\mathbf{Q}$ and $\mathbf{R}$ are positive definite $m \times m$ and $n \times n$ weighting

matrices, respectively. he matrix $\mathbf{F}$ contains the reference trajectory, such that

$$\mathbf{F} = -2 \cdot \mathbf{Q} \cdot \begin{bmatrix} x_r(0) \\ \vdots \\ x_r(N) \end{bmatrix} . \tag{19}$$

By selecting the state variable x as r_g and input signal u as the term $\ln \frac{F_\mathrm{p}}{F_\mathrm{s}} - \ln \frac{F_\mathrm{p}}{F_\mathrm{s}}|_{ss}$, the linearization of the nonlinear plant dynamics expressed in (12i) in discrete time is given by,

$$\mathcal{A}\mathbf{x} = \mathcal{B}\mathbf{u} + \mathcal{C} \,, \tag{20}$$

where we define,

$$\mathcal{A} = \begin{bmatrix} I & 0 & \dots & 0 \\ -A_o & I & \ddots & \vdots \\ \vdots & \ddots & \ddots & 0 \\ 0 & \dots & -A_{\mathrm{N}-1} & I \end{bmatrix}, \mathcal{B} = \begin{bmatrix} 0 & \dots & 0 \\ B_o & \ddots & \vdots \\ \vdots & \ddots & 0 \\ 0 & \dots & B_{\mathrm{N}-1} \end{bmatrix}, \mathcal{C} = \begin{bmatrix} x_o \\ C_o \\ \vdots \\ C_{\mathrm{N}-1} \end{bmatrix}, \tag{21a}$$

and A_k and B_k obtained to be,

$$A_k = 1 + \Delta t \cdot \left(2\,\omega_{\mathrm{p},k}\,\Delta\,\frac{1+\cos^2(\beta)}{\sin(2\beta)}(2c_1 x_\mathrm{k} + c_2)\,u_\mathrm{k} \right) \tag{21b}$$

$$B_k = \Delta t \cdot 2\,\omega_{\mathrm{p,k}}\,\Delta \frac{1+\cos^2(\beta)}{\sin(2\beta)}(c_1 x_\mathrm{k}^2 + c_2\ x_\mathrm{k} + c_3) \,, \tag{21c}$$

and additionally,

$$C_k = f(x_\mathrm{k}^i, u_\mathrm{k}^i) - (A_k\,x_\mathrm{k}^i + B_k\,u_\mathrm{k}^i) \,. \tag{21d}$$

Therefore, we can express $\mathbf{x}$ as function of $\mathbf{u}$ in a similar manner with MPC prediction matrix (Khalik, 2018),

$$\mathbf{x} = \mathbf{\Phi} + \mathbf{\Gamma}\mathbf{u} \,, \tag{22}$$

where $\Phi = \mathcal{A}^{-1}\mathcal{C}$ and $\Gamma = \mathcal{A}^{-1}\mathcal{B}$. This yields an elimination of x as a decision variable. Using this formulation, (15) can therefore be equivalently represented as:

$$\mathbf{u^{i+1}} = \underset{\mathbf{u}}{\operatorname{argmin}} \frac{1}{2}\mathbf{u}^\top \mathbf{Z}\mathbf{u} + \mathbf{G}^\top \mathbf{u} \,, \tag{23}$$

subject to:

$$\begin{bmatrix} \Gamma \\ -\Gamma \\ I \\ -I \end{bmatrix} \mathbf{u} \leq \begin{bmatrix} \overline{\mathbf{x}} - \Phi \\ \Phi - \underline{\mathbf{x}} \\ \overline{\mathbf{u}} \\ -\underline{\mathbf{u}} \end{bmatrix} \tag{24}$$

with the weight parameters given by,

$$\mathbf{Z} = \begin{bmatrix} \Gamma \\ I \end{bmatrix}^\top \mathbf{R} \begin{bmatrix} \Gamma \\ I \end{bmatrix} , \mathbf{G} = \begin{bmatrix} \Gamma \\ I \end{bmatrix}^\top \left(\mathbf{R} \begin{bmatrix} \Phi \\ 0 \end{bmatrix} + \mathbf{F} \right) . \tag{25}$$

Here, the state constraints $\overline{\mathbf{x}}$ and $\underline{\mathbf{x}}$ can be eliminated from the control objective formulation, as it is written to be a plant design constraint in (12g). Therefore, the combined plant and control optimization problem in (12a) can be reformulated as,

$$\underset{\mathbf{x_p},\mathbf{u}}{\operatorname{argmin}}\, w_\mathrm{p} M_v + w_c \left(\frac{1}{2}\mathbf{u}^\top \mathbf{Z}\mathbf{u} + \mathbf{G}^\top \mathbf{u} \right) , \tag{26}$$

subject to: (12b)-(12g) and $\begin{bmatrix} I \\ -I \end{bmatrix} \mathbf{u} \leq \begin{bmatrix} \overline{\mathbf{u}} \\ -\underline{\mathbf{u}} \end{bmatrix}$,

where the plant design parameters are chosen to be

$$\mathbf{x_p} = \{\beta, R_{1,\mathrm{p}}, R_{2,\mathrm{p}}, R_{1,\mathrm{s}}, R_{2,\mathrm{s}}\} \,,$$

and the control design parameters are the discretized input signal $\mathbf{u}$. Using this formulation, the nonlinear constraint in (12i) is replaced by (22). The input bounds are defined by the maximum and minimum allowable F_p,

$$\overline{u_\mathrm{k}} = \log\left(\frac{\overline{F_{\mathrm{p,k}}}}{F_{\mathrm{s,k}} \cdot \frac{F_\mathrm{p}}{F_\mathrm{s}}\big|_{\mathrm{ss}}} \right) , \underline{u_\mathrm{k}} = \log\left(\frac{\underline{F_{\mathrm{p,k}}}}{F_{\mathrm{s,k}} \cdot \frac{F_\mathrm{p}}{F_\mathrm{s}}\big|_{\mathrm{ss}}} \right) . \tag{27}$$

where $\overline{F_\mathrm{p}}$ and $\underline{F_\mathrm{p}}$ are the minimum and maximum allowable primary clamping forces, respectively. The maximum allowable clamping force is chosen to be a constant value. The minimum allowable clamping force depends on the primary torque,

$$\underline{F_\mathrm{p}} = \frac{S_\mathrm{f} \cdot |T_\mathrm{p}| \cdot \cos\beta}{2 \cdot \mu_\mathrm{cvt} \cdot R_\mathrm{p}} \,, \tag{28}$$

which is determined by the primary torque T_p and wedge angle β.

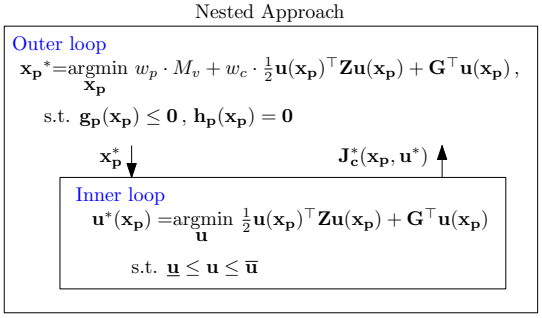

Fig. 3. Nested optimization approach for the combined plant and control design problem

4. RESULTS AND DISCUSSION

Here, the combined plant and control optimization for the application of a CVT system is proposed. The combined plant and control optimization formulation is solved using a nested/bi-level approach (Fig. 3). The reference trajectory for ratio tracking in this case is obtained from the WLTP drive cycle.

4.1 Trade-off between control effort and variator size

In this subsection, the results of solving the combined plant and control optimization problem are discussed. Here, we prioritize minimizing the tracking error over the control effort for the control problem by selecting $\mathbf{Q} = \mathbf{I}_{\mathrm{N}\times\mathrm{N}}$ and $\mathbf{R} = 0.1 \cdot \mathbf{I}_{\mathrm{N}\times\mathrm{N}}$. Furthermore, we will look at different pairs of w_p and w_c to investigate the trade-off between plant and

Table 2. Simulation parameters

parameter	description	value	unit
Δt	sampling time	0.5	s
$\overline{r_\mathrm{g}}$	max. ratio	2.85	-
$\underline{r_\mathrm{g}}$	min. ratio	0.35	-
$\overline{\beta}$	max. wedge angle	13	^{o}
$\underline{\beta}$	min. wedge angle	7	^{o}
$R_{1,min}$	Min. top radius	18.5	mm
$R_{2,min}$	Min. bottom radius	70	mm
$R_{1,max}$	Max. top radius	30	mm
$R_{2,max}$	Max. bottom radius	90	mm
$F_{p,max}$	Max. primary clamp. force	100	kN
δ_a	Min. center distance	3	mm
δ_{ou}	Dist. from pulley edge	4	mm
δ_{in}	Dist. from pulley edge	4	mm

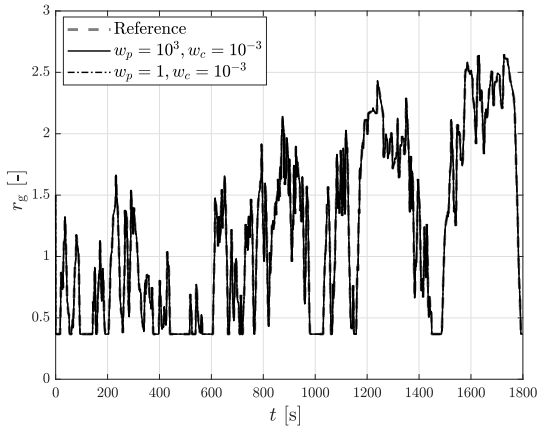

Fig. 4. Ratio tracking results for the WLTP cycle with $\mathbf{Q} = \mathbf{I}_{\mathrm{N}\times\mathrm{N}}$ and $\mathbf{R} = 0.1 \cdot \mathbf{I}_{\mathrm{N}\times\mathrm{N}}$

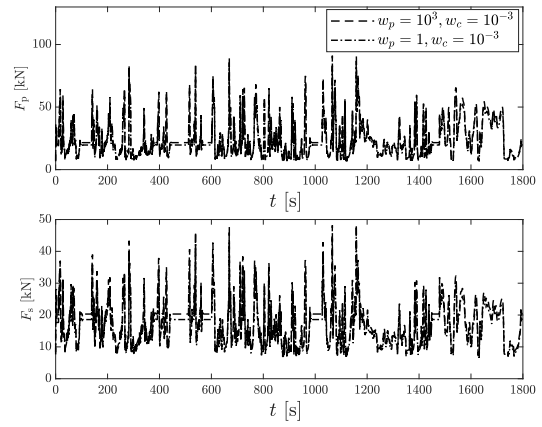

Fig. 5. Plot of clamping forces F_p and F_s with $\mathbf{Q} = \mathbf{I}_{\mathrm{N}\times\mathrm{N}}$ and $\mathbf{R} = 0.1 \cdot \mathbf{I}_{\mathrm{N}\times\mathrm{N}}$

Table 3. Results of Optimization for $\mathbf{Q} = \mathbf{I}_{\mathrm{N}\times\mathrm{N}}$ and $\mathbf{R} = 0.1 \cdot \mathbf{I}_{\mathrm{N}\times\mathrm{N}}$

parameter	description	benchmark	optimized	optimized	unit
w_p	opt. weight	-	10^3	1	-
w_c	opt. weight	-	10^{-3}	10^{-3}	-
J_p	plant objective	7.1	4.09	4.54	kg
J_c	control objective	280.74	1.29	1.29	–
β	wedge angle	11	7	7	^{o}
$R_{1,\mathrm{p}}$	inner radius	23.5	19.1	21.5	mm
$R_{2,\mathrm{p}}$	outer radius	85.5	70	72.6	mm
$R_{1,\mathrm{s}}$	inner radius	24	19.1	20	mm
$R_{2,\mathrm{s}}$	outer radius	86.5	70	77	mm
a	center distance	171	143	152.6	mm

control optimization, namely with $w_\mathrm{p} = 1$, $w_c = 10^{-3}$ and $w_\mathrm{p} = 10^3$, $w_c = 10^{-3}$. The results are depicted in Fig. 4 and Fig. 5. The detailed results are summarized in Table 3.

It can be seen in Fig. 4 that for both cases, the optimized plant designs are able to accurately follow the desired ratio trajectory $r_{\mathrm{g,r}}$. Nevertheless, optimizing for $w_\mathrm{p} = 10^3, w_\mathrm{p} = 10^{-3}$ yields a lower plant objective J_p, as shown in Table 3. Consequently, the design obtained with this set of weight yields higher required clamping forces F_p and F_s than that of $w_\mathrm{p} = 1$, $w_c = 10^{-3}$, as depicted in Fig. 5. This is because for the former, there is more emphasis on minimizing the plant objective , which in return yields higher required clamping forces to accurately track the desired ratio trajectory. The result indicates that there is a relationship between control effort and plant design.

4.2 Tradeoff between tracking error and control effort

Previous study in Subsection 4.1 showed the trade-off between the plant and control design problem. In this subsection, the results of using different weighting matrices $\mathbf{Q}, \mathbf{R}$ for the control optimization problem will be discussed. Here, we compare the results obtained by prioritizing minimization of control effort than tracking error. To demonstrate this, we will compare the results and performance of an optimized CVT with $\mathbf{Q} = 10^{-4} \cdot \mathbf{I}_{\mathrm{N}\times\mathrm{N}}, \mathbf{R} = \mathbf{I}_{\mathrm{N}\times\mathrm{N}}$ and $\mathbf{Q} = \mathbf{I}_{\mathrm{N}\times\mathrm{N}}, \mathbf{R} = 10^{-6} \cdot \mathbf{I}_{\mathrm{N}\times\mathrm{N}}$ for the control optimization formulation. The results are depicted in Fig. 6 and Fig. 7.

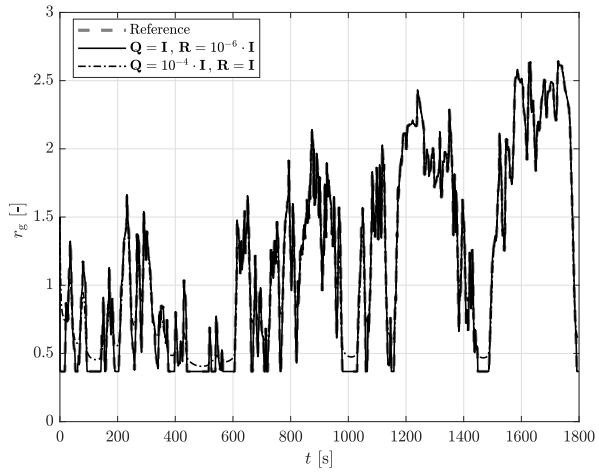

Fig. 6. Ratio tracking comparison between $\mathbf{Q} = 10^{-4} \cdot \mathbf{I}_{\mathrm{N}\times\mathrm{N}}$, $\mathbf{R} = \mathbf{I}_{\mathrm{N}\times\mathrm{N}}$ and $\mathbf{Q} = \mathbf{I}_{\mathrm{N}\times\mathrm{N}}$, $\mathbf{R} = 10^{-6} \cdot \mathbf{I}_{\mathrm{N}\times\mathrm{N}}$

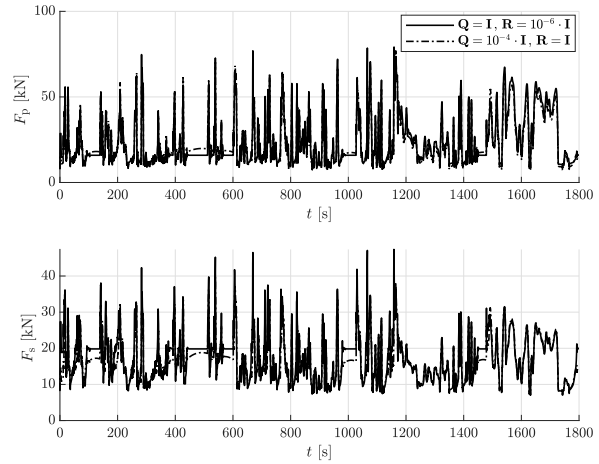

Fig. 7. Clamping forces comparison between $\mathbf{Q} = 10^{-4} \cdot \mathbf{I}_{\mathrm{N}\times\mathrm{N}}$, $\mathbf{R} = \mathbf{I}_{\mathrm{N}\times\mathrm{N}}$ and $\mathbf{Q} = \mathbf{I}_{\mathrm{N}\times\mathrm{N}}$, $\mathbf{R} = 10^{-6} \cdot \mathbf{I}_{\mathrm{N}\times\mathrm{N}}$

It can be seen from Fig. 6 that for $\mathbf{Q} = \mathbf{I}_{\mathrm{N}\times\mathrm{N}}$, $\mathbf{R} = 10^{-6} \cdot \mathbf{I}_{\mathrm{N}\times\mathrm{N}}$, better ratio tracking performance is achieved. Consequently, it is also shown that the required clamping

Table 4. Comparison of Results

parameter	description	optimized	optimized	unit
$\mathbf{Q}$	opt. weight	$\mathbf{I}_{\mathrm{N}\times\mathrm{N}}$	$10^{-4}\cdot\mathbf{I}_{\mathrm{N}\times\mathrm{N}}$	-
$\mathbf{R}$	opt. weight	$10^{-6}\cdot\mathbf{I}_{\mathrm{N}\times\mathrm{N}}$	$\mathbf{I}_{\mathrm{N}\times\mathrm{N}}$	-
J_{p}	plant objective	5	4.09	kg
J_{c}	control objective	1.28	0.012	–
β	wedge angle	12.7	7	^{o}
$R_{1,\mathrm{p}}$	inner radius	19.3	19.1	mm
$R_{2,\mathrm{p}}$	outer radius	70	70	mm
$R_{1,\mathrm{s}}$	inner radius	19.1	19.1	mm
$R_{2,\mathrm{s}}$	outer radius	70.6	70	mm
a	center distance	143	143	mm

forces for this pair of weighting factors are higher than those of $\mathbf{Q} = 10^{-4}\cdot\mathbf{I}_{\mathrm{N}\times\mathrm{N}}$ and $\mathbf{R} = \mathbf{I}_{\mathrm{N}\times\mathrm{N}}$. This is because by using this pair of weighting factors, the ratio tracking performance is relaxed, which allows the controller to reduce the control effort, and therefore the required clamping forces. Additionally, as shown in Table 4, even with the same values of w_p and w_c, the combined plant and control optimization results in different sets of design parameters. This shows that there is a trade-off between minimizing the control effort and the resulting ratio tracking error.

5. CONCLUSIONS AND FUTURE WORK

Based on the study, it is concluded that the current CVT variator design can be reduced in terms of size and weight while still being able to follow the desired ratio trajectory provided in this work. Furthermore, it can be observed from the results that the selected weighting parameters of the proposed control optimization problem can influence the results of the combined plant and control design problem.

In the future, the optimized design will be evaluated for more aggressive driving behaviours, as well as the resulting energy efficiency of the CVT. Moreover, analyzing the benefits of redesigning the CVT for a specific powertrain topology i.e., energy consumption, cost, performance, can be done as an extension of this study.

REFERENCES

H.K. Fathy, Combined Plant And Control Optimization: Theory, Strategies and Applications. *PhD Thesis*, University of Michigan, 2003.

H.K. Fathy, J.A. Reyer, P.Y. Papalambros, A.G. Ulsoy, On the Coupling between the Plant and Controller Optimization Problems. *Proceedings of the American Control Conference*, Arlington, VA, 2001.

D.L. Peters, P.Y. Papalambros, and A.G. Ulsoy, On Measures of Coupling Between the Artifact and Controller Optimal Design Problems. *Proceedings of the ASME Design Engineering Technical Conferences*, San Diego, CA, 2009.

D.R. Herber, J.T. Allison, Nested and Simultaneous Solution Strategies for General Combined Plant and Control Design Problems. *Journal of Mechanical Design*, 2018.

L.V. Pérez, G.R. Bossio, D. Moitre, G.O. Garcia, Optimization of power management in a hybrid electric vehicle using dynamic programming. *Mathematics and Computers in Simulation*, volume 73, 2006.

O. Sundström, L. Guzzella, P. Soltic, Optimal Hybridization in Two Parallel Hybrid Electric Vehicles using Dynamic Programming. *IFAC Proceedings*, volume 41, pages 4642–4647, 2008.

E. Silvas, E. Bergshoeff, T. Hofman, M. Steinbuch, Comparison of Bi-Level Optimization Frameworks for Sizing and Control of a Hybrid Electric Vehicle. *IEEE Vehicle Power and Propulsion Conference (VPPC)* , 2014.

Bellman. Dynamic Programming. *USA: Princeton Univ. Press*, 1957.

C.A. Fahdzyana, T. Hofman. Integrated design for a CVT: dynamical optimization of actuation and control. *IFAC Conference on Advances in Automotive Control (AAC)*, 2019.

C.A. Fahdzyana, T. Hofman. Joined Plant and Control Design for Continuous Variable Transmission Systems *American Control Conference (ACC)*, 2020.

G. Carbone, L. Mangialardi, G. Mantriota, The Influence of Pulley Deformations on the Shifting Mechanism of Metal Belt CVT. *Journal of Mechanical Design*, vol. 127, 2005.

S. van der Meulen. High-performance Control of Continuously Variable Transmissions. *PhD Thesis*, Eindhoven University of Technology, 2010.

K. van Berkel. Control of a mechanical hybrid powertrain. *PhD Thesis*, Eindhoven University of Technology, 2013.

B.G. Vroemen. Component control for the Zero Inertia powertrain. *PhD Thesis*, Eindhoven University of Technology, 2001.

B. Bonsen. Efficiency optimization of the push-belt CVT by variator slip control. *PhD Thesis*, Eindhoven University of Technology, 2006.

A. Brandsma, J. van Lith, E. Hendriks. Push belt CVT developments for high power applications. *International Congress on Continuously Variable Power Transmission*, 1999.

Z. Khalik, G.P. Padilla, T.C.J. Romijn, M.C.F. Donkers. Vehicle energy management with ecodriving. *American Control Conference (ACC)*, 2018.

J. Nocedal S. J. Wright. Numerical Optimization. *Springer*, 2006.